Journal of Applied Physics

Nanoparticle-based metasurfaces for angular independent spectral filtering applications

Cite as: J. Appl. Phys. **126**, 213101 (2019); https://doi.org/10.1063/1.5108578
Submitted: 02 May 2019 . Accepted: 11 November 2019 . Published Online: 02 December 2019

Francesco Lotti, Ali Mirzaei, Andrey E. Miroshnichenko, and Anatoly V. Zayats

AIP Publishing

Nanoparticle-based metasurfaces for angular independent spectral filtering applications

Cite as: J. Appl. Phys. **126**, 213101 (2019); doi: 10.1063/1.5108578
Submitted: 2 May 2019 · Accepted: 11 November 2019 ·
Published Online: 2 December 2019

View Online Export Citation CrossMark

Francesco Lotti,[1,a)] Ali Mirzaei,[2] Andrey E. Miroshnichenko,[3] and Anatoly V. Zayats[1]

AFFILIATIONS

[1]Department of Physics, King's College London, Strand, London WC2R 2LS, United Kingdom
[2]Nonlinear Physics Centre, Research School of Physics and Engineering Australian National University, Canberra ACT 2601, Australia
[3]School of Engineering and Information Technology, University of New South Wales, Canberra ACT 2600, Australia

Note: This paper is part of the Special Topic on Dielectric Nanoresonators and Metamaterials.
[a)]**Electronic mail:** francesco.lotti@kcl.ac.uk

ABSTRACT

We designed a metasurface made of a monolayer of spherical nanoparticles embedded in a dielectric slab, which exhibits transmission properties independent of the incidence angle. Adjusting the electromagnetic coupling between high-index dielectric and hybrid core-shell nanoparticles enables the metasurface to operate in low-pass, bandpass, as well as band-stop regimes in the visible and near-infrared spectral ranges. We demonstrate how symmetric properties of spherical nanoparticles determine the response of the metasurface, resulting in a spectral filter with a wide angular acceptance range. We study transmission characteristics of the metasurface, such as frequency selectivity, the slope of filtering at cutoff frequencies, and the robustness of the metasurface against experimental variations in geometrical parameters. Our analyses show that the proposed approach can be used to design angular-independent spectral filters with the same material platform and approach to operate in different regimes and spectral ranges.

I. INTRODUCTION

Going beyond natural optical materials, metamaterials are attracting attention in various photonic applications, providing flexibility to design optical response otherwise difficult to achieve. This has become possible by introducing meta-atoms as building blocks of metamaterial structures. Similar to natural materials, the geometry and properties of meta-atoms and their arrangement and topology determine the properties of the metamaterials.[1–4] Various designs of meta-atoms have been introduced for different applications, such as invisibility cloaking[5] and optical nonlinearity engineering.[6] However, among studied meta-atoms, the symmetry of spherical nanoparticles provides with isotropic optical response based on strong multipolar resonances. The use of such meta-atoms in metamaterials in general[7–10] and metasurfaces in particular has led to highly efficient structures with tuneable response[11–13] and controlled reflectivity[14] and streamlined nanoantenna designs.[15] The simple structure of spherical meta-atoms has led to a better understanding of their interaction with light in terms of polarization[16–18] and absorption[19–23] control in nanosphere-based metastructures.

Transmissive metasurfaces have recently received much attention with various application oriented designs.[16,24–26] The dependence of the transmittance on the angle of incidence in gigahertz[27–29] and optical[30] spectral ranges has been studied; however, an angle-independent metasurface remains a challenge. In this work, we introduce an ultrathin, symmetrical metasurface for angular-independent spectral filtering. We use silicon spherical nanoparticles with and without plasmonic coating, capable of supporting resonant modes[31] immersed in a slab made of technologically relevant silicon nitride. Using the interplay between the resonant modes of the nanoparticles and the Fabry-Pérot mode of the slab, we demonstrate that the proposed metasurfaces maintain their transmission properties throughout a wide range of incidence angle. They make possible to construct broadband, frequency selective, low- or bandpass filters and narrowband sharp-notch filters, simply by modifying the nanosphere geometrical parameters and material and their spacing. The combination of Si nanoparticles and Au or TiN plasmonic shells, together with a high refractive index of the SiN host, allows designing the required spectral response throughout visible and near-infrared spectral ranges.

II. RESULTS AND DISCUSSION

The proposed design is schematically shown in Fig. 1(a) on the example of a planar array of silicon nanoparticles coated with a gold shell inside a dielectric slab. We employed a Finite Element Method using the commercial software CST-Studio to analyze the optical properties of the metasurfaces with different geometrical parameters. The filter response to both the transverse magnetic (TM) and transverse electric (TE) polarized incident light, as well as to unpolarized light, important for practical applications, was examined. Experimental data on the permittivity of various materials were taken from Refs. 32 and 33. The simulations were performed by defining a unit cell which includes one spherical nanoparticle embedded in the dielectric slab and using a two-dimensional periodic boundary condition. Due to reciprocity, the transmission spectrum is symmetric from both sides of the metasurface and can be evaluated using the scattering matrix ($|S_{21}|^2$).[34]

The general operation principle of the proposed metasurface-based optical filter is determined by the interplay of resonant transmission of a dielectric slab and the resonant absorption and scattering of the nanoparticle. This is demonstrated in Fig. 1(c) which shows the spectral behavior of a single silicon nanoparticle of a radius 60 nm in an infinite high-refractive-index medium (SiN) and the transmission spectra of the SiN slab.

Due to their small size compared to the operating wavelength, isolated nanoparticles support two modes only (electric and magnetic dipoles), and the excitation of higher-order multipoles is negligible. These two modes might scatter light in a certain angular pattern, thus decreasing the overall transmitted light. Furthermore, part of the scattered light is reflected back at the dielectric-air surface, remaining in the slab and feeding the nearby nanoparticles. At the wavelengths out of resonance, the incident light sees a medium whose effective refractive index is an average between the one of the slab and that of the nanoparticles and passes through the metasurface otherwise unimpeded. Depending on a distance between the nanoparticles and the nature of the resonances, e.g., plasmonic, dielectric or core-shell nanoparticles, the coupling between the nanoparticles may play a role in determining the filter characteristics, including overall transmission and spectral position and sharpness of the filtering slope. The metasurface-based optical filters can be designed to achieve various types of spectral filtering, such low-pass, band-path, and band-stop filters.

Low-pass filtering can be achieved using an array of Si nanoparticles in a SiN slab (Fig. 2). The transmission spectra for TE- and TM-polarized light as well as unpolarized light confirm that the symmetrical properties of spherical nanoparticles lead to angular-independent transmission of the metasurface. The gap between the nanospheres, their radius, and the thickness of the slab are playing different roles in the filtering properties. Changing only the radius of nanoparticles from 30 nm to 60 nm allows us to tune the transmission spectrum in a wide spectral range from below 400 nm to beyond 500 nm with larger nanospheres naturally leading to longer wavelength cutoff in the long-pass regime [Fig. 2(d)].

The relatively low density of the nanoparticles considered in the design ensures high transmittance in the transparency bands, but it is sufficient to achieve strong suppression of the transmitted light in the rejection bands. At the inter-particle distances larger than 10 nm, the interaction between the nanoparticles is weak [Fig. 2(b)], and the optical response is determined by the interplay between the resonances of individual nanoparticles and the Fabry-Pérot modes of the supporting slab. This makes the design robust against the disorder in the array of the nanoparticles. On the other hand, the dispersion in nanoparticle sizes is more important in this design. The different sizes lead to different cutoff wavelengths [Fig. 2(d)]. Therefore, the distribution of sizes

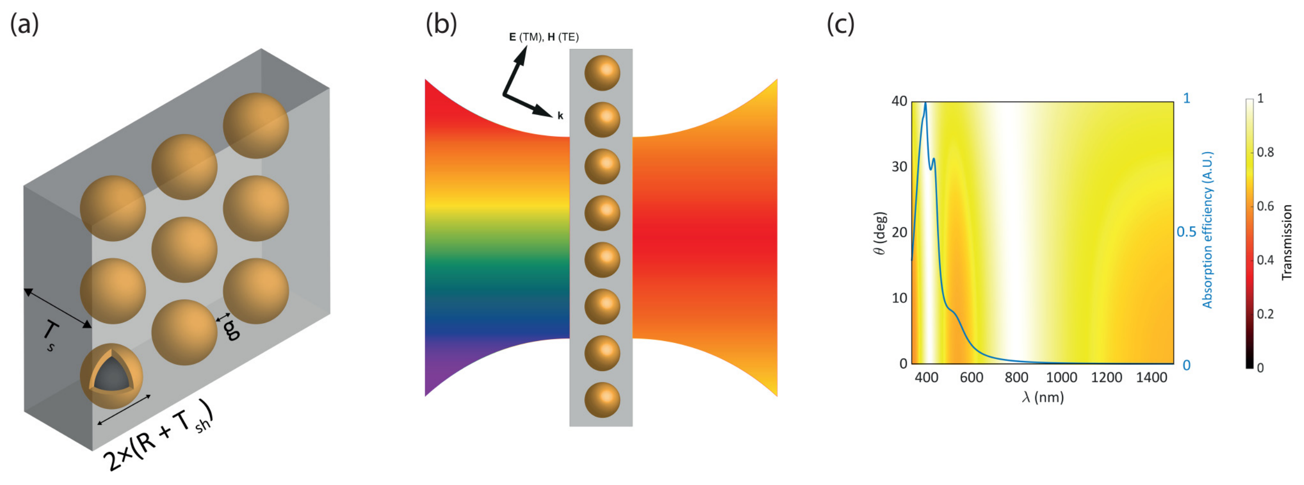

FIG. 1. (a) Schematic view of a metasurface made of spherical nanoparticles inside a dielectric layer. The parameters of the model (radius of the nanoparticles, R, separation between nanoparticles, g, and the slab thickness, T_s, are indicated. (b) Illustration of the spectral filter based on a metasurface. (c) Parametric plot of the transmission of a dielectric slab ($T_s = 200$ nm, refractive index n = 2.2) without nanoparticles superimposed with the absorption spectrum of a single silicon nanoparticle with R = 60 nm (solid line).

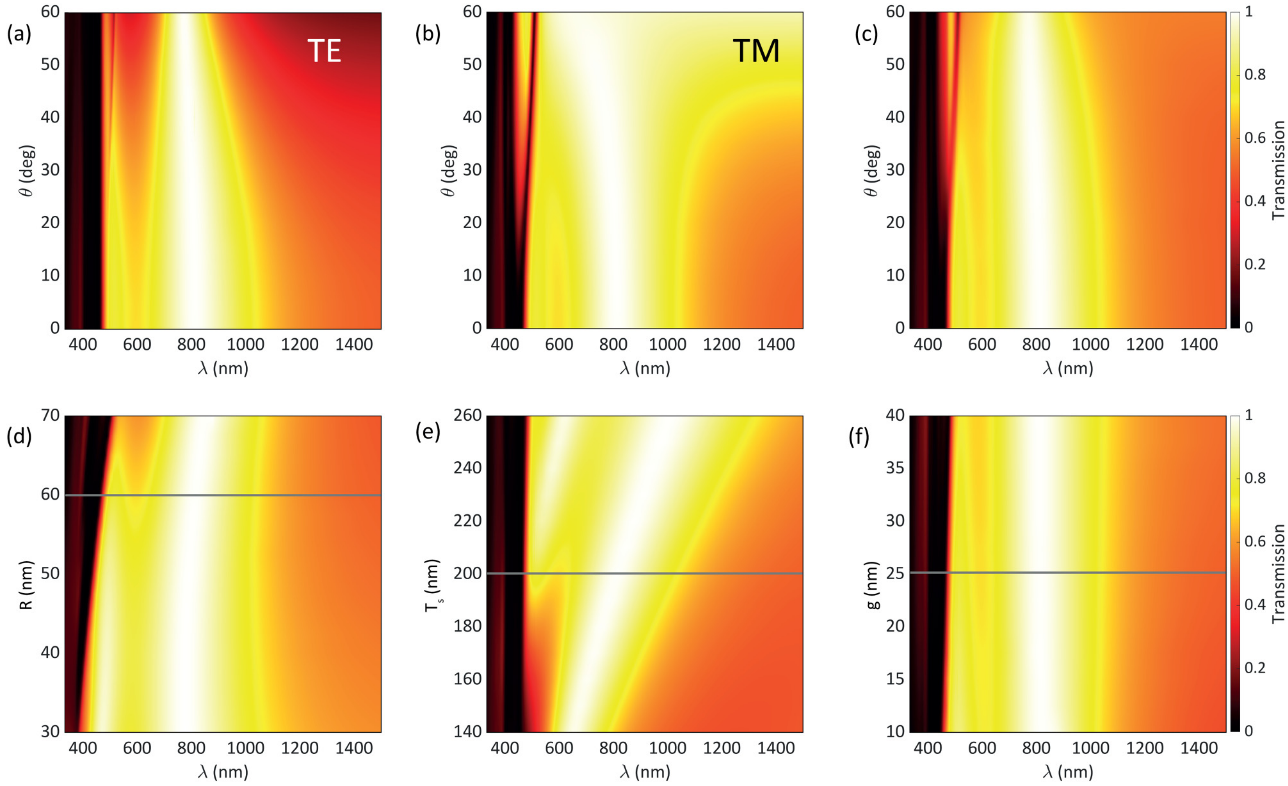

FIG. 2. The transmission spectra of the metasurface based on an array of Si nanoparticles in a dielectric slab (R = 60 nm, g = 25 nm, T_s = 200 nm) for (a) TE-polarized, (b) TM-polarized light and (c) unpolarized light. (d)–(f) Transmission spectra dependence on (d) radius, R, (e) separation, g, and (f) slab thickness, T_s, at normal incidence. The other parameters of the metamaterial are the same as in (a). The gray lines indicate the same parameters in different plots. The color scale is the same for all plots.

of the nanoparticles leads to the broadening of the filtering slope. For example, for a Gaussian distribution of sizes around 50 nm radius, the transmission is increased in the stop band below 0.1 [Fig. 3(a)].

The small variations of the slab thickness allow efficient tuning of the spectral filtering slope of the pass/stop band boundary without strongly influencing the stop band range. By decreasing the thickness of the slab, the slope of filtering gradually

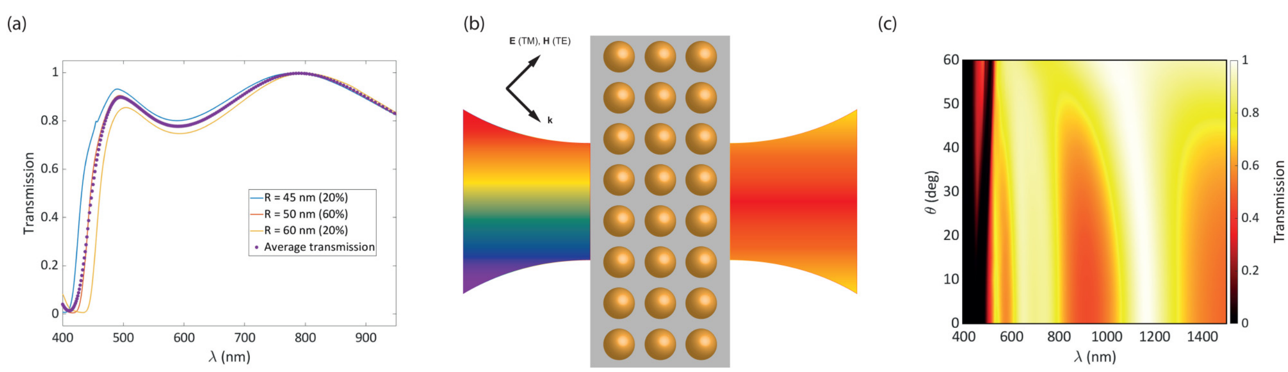

FIG. 3. (a) The transmission spectra of the metasurface as in Fig. 2(a) for a Gaussian distribution of the nanoparticle sizes around R = 50 nm at normal incidence. (b) Schematics of the filter with three layers of nanoparticles [cf. Fig. 1(b)]. The particles form a primitive cubic lattice with g = 25 nm in both directions. (c) Transmission spectra of the design in (b) for different angles of incidence for TM-polarized light. The slab thickness is 515 nm; all other parameters are as in Fig. 2(a).

becomes smoother [Fig. 2(e)]. However, for significantly different thicknesses of the slab, the free spectral range of the Fabry-Pérot cavity changes, which may lead to strong changes of the transmission spectrum.

It is instructive to compare the single layered and multilayered designs of the filters, with particles forming a primitive cubic lattice [Fig. 3(b)]. If the separation between the nanoparticles is too large for the interaction between the resonances to be significant and, on the other hand, too small for the photonic crystal effects to appear, the difference in the filtering properties comes from different Fabry-Pérot resonances of the slab, whose thickness is significantly increased to accommodate the multilayer [Fig. 3(c)]. The optical response of the nanoparticles is not changed for a multilayer as it is governed by the resonances of individual nanoparticles. The major difference is the free spectral range of the thicker Fabry-Pérot cavity, which is smaller, therefore, the structure exhibits another transmission line. This opens up the possibility of using multilayered systems as an additional degree of freedom, in expense of fabrication feasibility. Similar considerations on the disorder of actual structures hold for the other filters discussed in this work. These results show a high degree of flexibility in the design of reliable angle-independent metasurfaces for low-pass filtering applications by the possibility of precise tuning in a wide spectral range.

A. Bandpass filters

Adding a shell over silicon nanoparticles leads to the spectral shift of the excited modes which has been discussed in detail in previously reported studies.[35,36] A plasmonic shell over silicon particles excites localized surface plasmons[37,38] so that the interaction between the nanoparticles becomes stronger and plays a more complicated role in the metasurface filter response. As the result, the stop band appears, which leads to the formation of a well defined passband in the spectral range between 600 and 800 nm [Figs. 4(a) and 4(b)]. This hybrid plasmonic-dielectric metasurface preserves the transmission independence of the angle of incidence for both TM- and TE- polarizations. The field distribution of the electric field inside the slab clearly shows the differences in the pass band and the stop bands on its edges (Fig. 5). The symmetric field distribution ensures strong transmission, while asymmetric field distribution corresponds to the stop band when transmission is significantly suppressed.

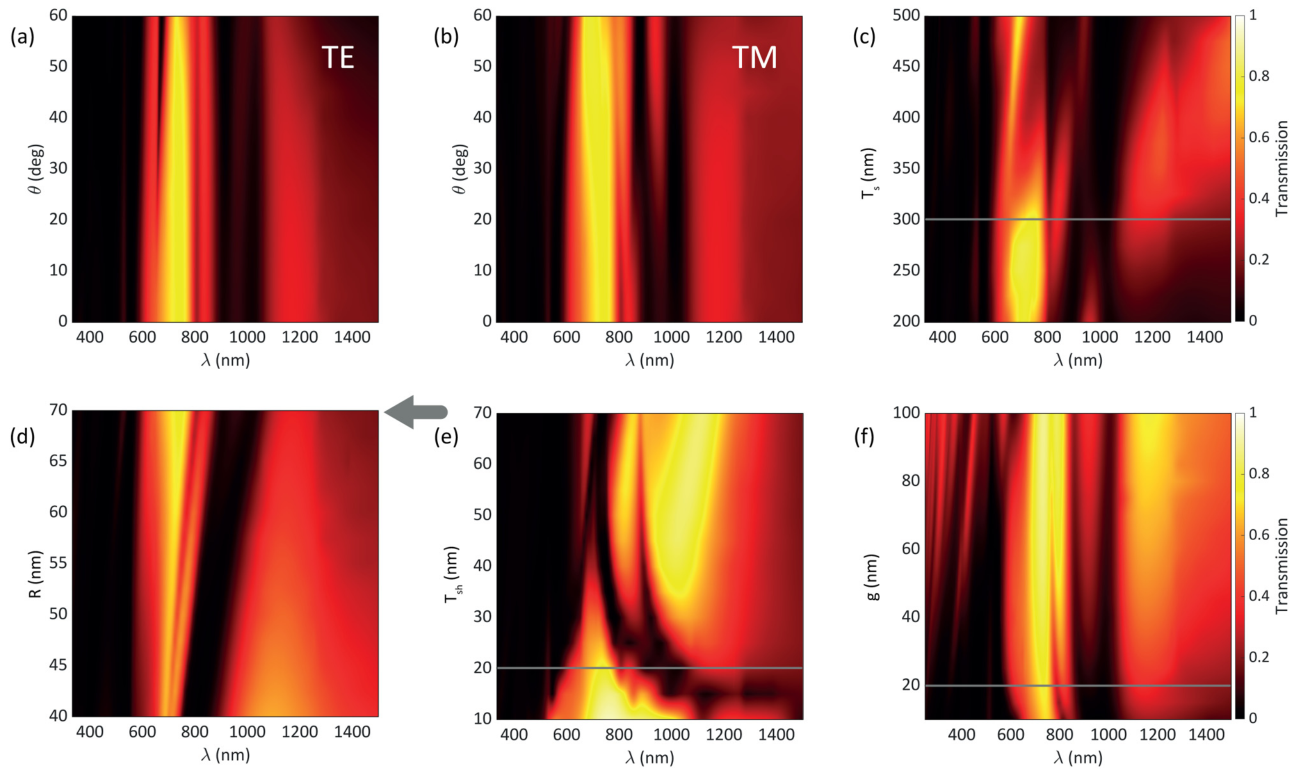

FIG. 4. Transmission of a metasurface based on Si nanoparticles (core radius $R_c = 70$ nm) coated with gold shell ($T_{sh} = 20$ nm), arranged in the array with $g = 20$ nm in the SiN slab with $T_s = 300$ nm for (a) TE- and (b) TM- polarized light. (c)–(f) Transmission spectra dependence on (c) slab thickness, T_s, (d) radius of Si core, R_c, (e) Au shell thickness, T_{sh}, and (f) separation, g, at normal incidence. The other parameters of the metamaterial are the same as in (a). The gray lines indicate the same parameters in different plots. The color scale is the same for all plots.

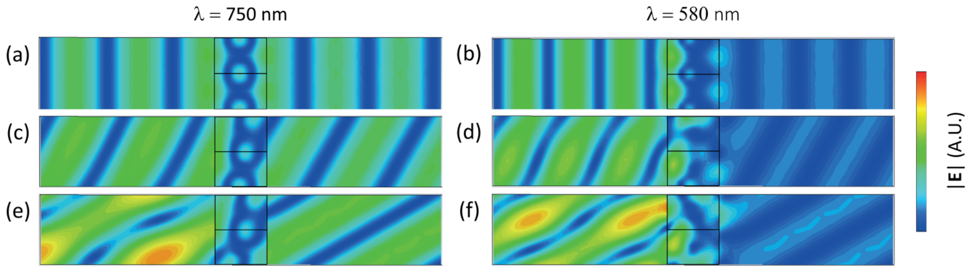

FIG. 5. Electric field distributions in and around the filter for TM-polarized light at the incidence angles of (a) and (b) 0°, (c) and (d) 30°, and (e) and (f) 60° for (a), (c), (e) bandpass and (b), (d), (f) band-stop regimes. The metasurface parameters are as in Fig. 4(a).

The increase of the slab thickness results in a transition from wide to narrow bandpass properties at around $T_s = 300$ nm [Fig. 4(c)]. At the same time, when the core-radius, R_c, increases, the first cutoff wavelength stays constant, while the second one redshifts, therefore, allowing for a control of the bandwidth [Fig. 4(d)]. Using the additional degree of freedom in the core-shell nanoparticles, the thickness of the gold shell, T_{sh}, can be used to revert to a bandpass filter with the cutoff in the infrared region [Fig. 4(e)]. Finally, the distance between the core-shell nanoparticles, affecting a coupling between them, allows to shift the transmission range toward the UV wavelengths [Fig. 4(f)]. Overall, the effect of the coupling can be seen as the generation of two modes, one of which stays constant and the other shifts in the deep UV range. As the nanoparticles are further separated, the coupling becomes less important, and the modes converge to each other.

Additionally to the considered above core-shell particles, other multishelled designs with either dielectric or plasmonic core can be used to achieve the required transmission characteristics.

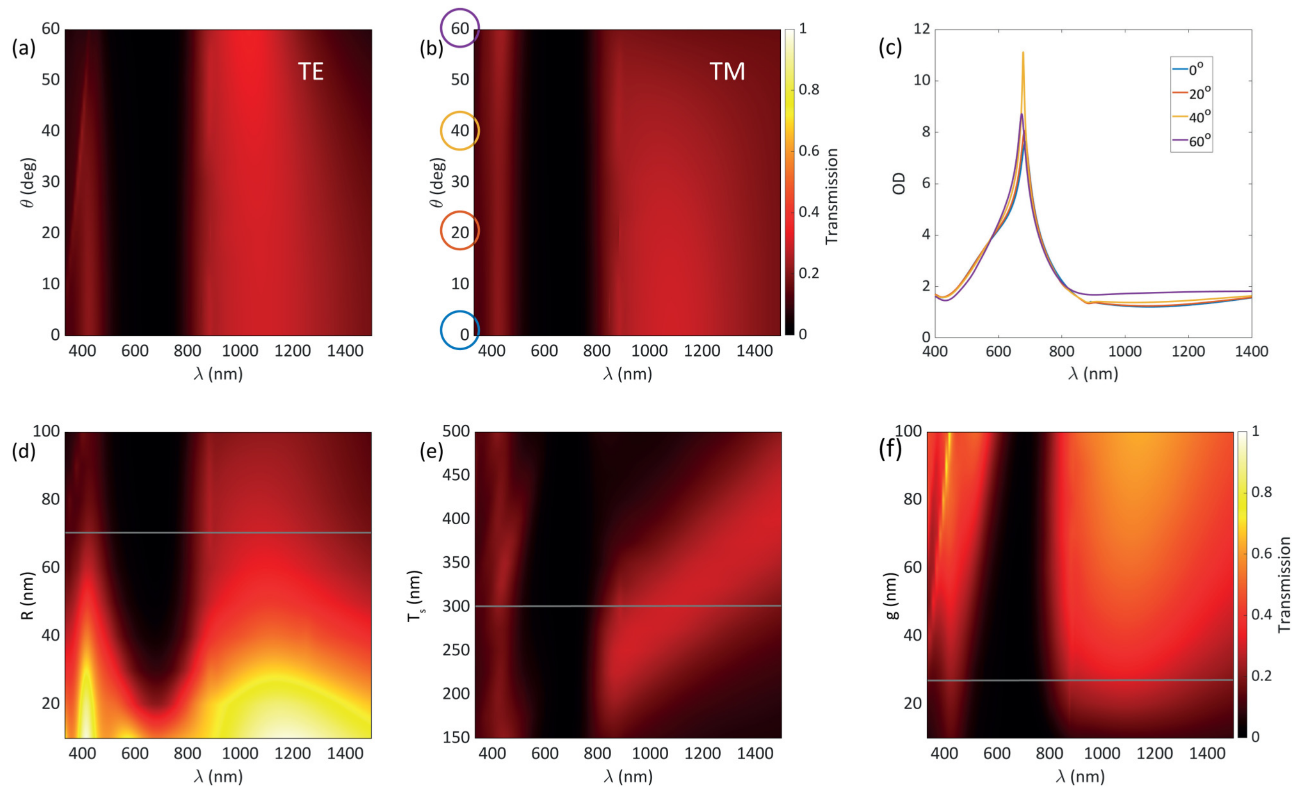

FIG. 6. Transmission of a metasurface based on TiN nanoparticles (R = 70 nm, g = 25 nm) in a SiN slab with $T_s = 300$ nm for (a) TE- and (b) TM-polarized light. (c) Spectra of the optical density for TM-polarized light for four selected angles [highlighted in (b)]. (d)–(f) Transmission spectra dependence on (d) radius of TiN nanoparticles, R, (e) slab thickness, T_s, and (f) separation, g, at normal incidence. The other parameters of the metamaterial are the same as in (a). The gray lines indicate the same parameters in different plots. The color scale is the same for all plots.

B. Band-stop filters

In the case of band-stop filters, the filter configuration was designed consisting of one layer of TiN nanoparticles in a SiN slab (Fig. 6). The Fabry-Pérot resonance determines the passband behavior and stop bands are determined by the nanoparticle resonance. TiN has been shown as a proper plasmonic ceramic with significant physical and chemical stability and biocompatibility. Moreover, its high melting temperature (close to 2800 °C) makes it an appropriate candidate for high temperature applications instead of commonly used plasmonic noble metals.[39] Using TiN particles, the omnidirectional band-stop and notch filers can be designed and optimized [Fig. 6(a) and 6(b)]. The spectra of the optical density, i.e., $-log_{10}$(Transmission), highlight the angular independence and sharpness of the absorption peak [Fig. 6(c)]. The transmission spectrum maintains the same filtering slope for most of the angles of incidence for the cutoff wavelengths on both sides of the stop band. The design can be adjusted to achieve the required width of the stop band [Fig. 6(d)]. Smaller radii of TiN nanoparticles lead to a narrower stop band with higher transmission in the pass-bands around it, at the expense of a lower suppression in the stop band. The same trade-off between the filtering quality and higher transmission in the pass-bands can be achieved by varying the separation between the nanoparticles in the array [Fig. 6(f)].

III. CONCLUSION

We introduced incident-angle-independent optical metasurface filters, based on a layer of nanoparticles in a high-refractive-index dielectric slab. We studied various examples of spectral filters employing silicon, gold, and titanium nitride nanoparticles in solid and core-shell realizations. The designed metastructures exhibit a variety of transmission properties, such as low-pass and band-pass as well as band-stop and notch filtering and are resilient against disorder. In the proposed design with a low density of the nanoparticles required to maintain high transmission, the interaction between the nanoparticles is weak, and the filter characteristics are determined by the resonances of individual particles and their interplay with the Fabry-Pérot modes of the slab where the nanoparticles placed. We demonstrated that it is possible to design filters for given cutoff frequencies in a wide range of optical wavelengths by choosing the required values of the design parameters. The effect of all the parameters of the metastructure, such as a core radius, a thickness of a shell and a slab, and a gap size, on the metasurface functionality in the suggested filtering regimes has been analyzed, such that one can use similar recipes to design a metasurface filter for a specific application. The functionality of the filters is practically independent of the separation between the nanoparticles in the array for larger distances, which indicates robustness against variations of the periodicity of the array in experimental realizations. At the same time, care should be taken to limit the size distribution of nanoparticles, which determine the sharpness of the transmission/rejection bands. The introduced metasurface filters exhibit high flexibility of the design and can engineered based on the requirements and expected filtering properties for a wide range of applications.

ACKNOWLEDGMENTS

This work was supported by the Defence Science and Technology Laboratory (DSTL), (Engineering and Physical Sciences Research Council (EPSRC), Australian Research Council, and the Europe-Asia-Pacific research program Nanophi. The authors thank Francisco Rodriguez Fortuño for useful discussions about the CST software. The data availability statement: all the data supporting this research are presented in the text and figures.

REFERENCES

[1]N. I. Zheludev and Y. S. Kivshar, "From metamaterials to metadevices," Nat. Mater. **11**, 917–924 (2012).
[2]N. Meinzer, W. L. Barnes, and I. R. Hooper, "Plasmonic meta-atoms and metasurfaces," Nat. Photonics **8**, 889–898 (2014).
[3]K. Tsai, G. A. Wurtz, J. Chu, T. Cheng, H. Wang, A. V. Krasavin, J. He, B. M. Wells, V. A. Podolskiy, J. Wang, Y. Wang, and A. V. Zayats, "Looking into meta-atoms of plasmonic nanowire metamaterial," Nano Lett. **14**, 4971–4976 (2014).
[4]I. Shadrivov, Y. Kivshar, and M. Lapine, *Nonlinear, Tunable and Active Metamaterials* (Springer International Publishing, 2015), Vol. 200.
[5]A. Alù and N. Engheta, "Achieving transparency with plasmonic and metamaterial coatings," Phys. Rev. E **72**, 016623 (2005).
[6]A. D. Neira, G. A. Wurtz, P. Ginzburg, and A. V. Zayats, "Ultrafast all-optical modulation with hyperbolic metamaterial integrated in Si photonic circuitry," Opt. Express **22**, 10987 (2014).
[7]B. Luk'yanchuk, N. I. Zheludev, S. A. Maier, N. J. Halas, P. Nordlander, H. Giessen, and C. T. Chong, "The Fano resonance in plasmonic nanostructures and metamaterials," Nat. Mater. **9**, 707–715 (2010).
[8]H. Alaeian and J. A. Dionne, "Plasmon nanoparticle superlattices as optical-frequency magnetic metamaterials," Opt. Express **20**, 15781–15796 (2012).
[9]W. Lewandowski, M. Fruhnert, J. Mieczkowski, C. Rockstuhl, and E. Górecka, "Dynamically self-assembled silver nanoparticles as a thermally tunable metamaterial," Nat. Commun. **6**, 6590 (2015).
[10]M. J. Smith, B. T. Kuhlmey, C. M. De Sterke, C. Wolff, M. Lapine, and C. G. Poulton, "Electrostriction enhancement in metamaterials," Phys. Rev. B Condens. Matter Mater. Phys. **91**, 1–7 (2015).
[11]K. Chen, B. B. Rajeeva, Z. Wu, M. Rukavina, T. D. Dao, S. Ishii, M. Aono, T. Nagao, and Y. Zheng, "Moiré nanosphere lithography," ACS Nano **9**, 6031–6040 (2015).
[12]Z. Wu, K. Chen, R. Menz, T. Nagao, and Y. Zheng, "Tunable multiband metasurfaces by moiré nanosphere lithography," Nanoscale **7**, 20391–20396 (2015).
[13]H. Ni, M. Wang, H. Hao, and J. Zhou, "Integration of tunable two-dimensional nanostructures on a chip by an improved nanosphere lithography method," Nanotechnology **27**, 225301 (2016).
[14]P. C. Li and E. T. Yu, "Flexible, low-loss, large-area, wide-angle, wavelength-selective plasmonic multilayer metasurface," J. Appl. Phys. **114**, 133104 (2013).
[15]A. Nemiroski, M. Gonidec, J. M. Fox, P. Jean-Remy, E. Turnage, and G. M. Whitesides, "Engineering shadows to fabricate optical metasurfaces," ACS Nano **8**, 11061–11070 (2014).
[16]A. Arbabi, Y. Horie, M. Bagheri, and A. Faraon, "Dielectric metasurfaces for complete control of phase and polarization with subwavelength spatial resolution and high transmission," Nat. Nanotechnol. **10**, 937 (2015).
[17]R. Paniagua-Domínguez, Y. F. Yu, A. E. Miroshnichenko, L. A. Krivitsky, Y. H. Fu, V. Valuckas, L. Gonzaga, Y. T. Toh, A. Y. S. Kay, B. Lukyanchuk, and A. I. Kuznetsov, "Generalized Brewster effect in dielectric metasurfaces," Nat. Commun. **7**, 10362 (2016).
[18]J. Jin, J. Luo, X. Zhang, H. Gao, X. Li, M. Pu, P. Gao, Z. Zhao, and X. Luo, "Generation and detection of orbital angular momentum via metasurface," Sci. Rep. **6**, 1–7 (2016).

[19]S. A. Tretyakov and S. I. Maslovski, "Thin absorbing structure for all incidence angles based on the use of a high-impedance surface," Microw. Opt. Technol. Lett. **38**, 175–178 (2003).
[20]H. Tao, C. M. Bingham, A. C. Strikwerda, D. Pilon, D. Shrekenhamer, N. I. Landy, K. Fan, X. Zhang, W. J. Padilla, and R. D. Averitt, "Highly flexible wide angle of incidence terahertz metamaterial absorber: Design, fabrication, and characterization," Phys. Rev. B Condens. Matter Mater. Phys. **78**, 2–5 (2008).
[21]J. Dai, F. Ye, Y. Chen, M. Muhammed, M. Qiu, and M. Yan, "Light absorber based on nano-spheres on a substrate reflector," Opt. Express **21**, 6697–6706 (2013).
[22]P. Feng, W. Li, and W. Zhang, "Dispersion engineering of plasmonic nanocomposite for ultrathin broadband optical absorber," Opt. Express **23**, 2328–2338 (2015).
[23]Y. Ra'Di, V. S. Asadchy, S. U. Kosulnikov, M. M. Omelyanovich, D. Morits, A. V. Osipov, C. R. Simovski, and S. A. Tretyakov, "Full light absorption in single arrays of spherical nanoparticles," ACS Photonics **2**, 653–660 (2015).
[24]J. Lin, P. Genevet, M. A. Kats, N. Antoniou, and F. Capasso, "Nanostructured holograms for broadband manipulation of vector beams," Nano Lett. **13**, 4269–4274 (2013).
[25]D. Lin, P. Fan, E. Hasman, and M. L. Brongersma, "Dielectric gradient metasurface optical elements," Science **345**, 298–302 (2014).
[26]S. Vo, D. Fattal, W. V. Sorin, Z. Peng, T. Tran, M. Fiorentino, and R. G. Beausoleil, "Sub-wavelength grating lenses with a twist," IEEE Photonics Technol. Lett. **26**, 1375–1378 (2014).
[27]J. A. Gordon, C. L. Holloway, and A. Dienstfrey, "A physical explanation of angle-independent reflection and transmission properties of metafilms/metasurfaces," IEEE Antennas Wirel. Propag. Lett. **8**, 1127–1130 (2009).
[28]K. Wang, J. Zhao, Q. Cheng, D. S. Dong, and T. J. Cui, "Broadband and broad-angle low-scattering metasurface based on hybrid optimization algorithm," Sci. Rep. **4**, 5935 (2014).
[29]D. Zaluški, A. Grbic, and S. Hrabar, "Analytical and experimental characterization of metasurfaces with normal polarizability," Phys. Rev. B **93**, 155156 (2016).
[30]Z. Li and K. Aydin, "Broadband metasurfaces for anomalous transmission and spectrum splitting at visible frequencies," EPJ Appl. Metamater. **2**, 2 (2015).
[31]A. I. Kuznetsov, A. E. Miroshnichenko, M. L. Brongersma, Y. S. Kivshar, and B. Luk'yanchuk, "Optically resonant dielectric nanostructures," Science **354**, aag2472 (2016).
[32]D. Aspnes and A. Studna, "Dielectric functions and optical parameters of Si, Ge, GaP, GaAs, GaSb, InP, InAs, and InSb from 1.5 to 6.0 eV," Phys. Rev. B **27**, 985 (1983).
[33]E. D. Palik, *Handbook of Optical Constants of Solids* (Academic Press, 1998), Vol. 3.
[34]B. E. Saleh and M. C. Teich, *Fundamentals of Photonics* (John Wiley & Sons, 2019).
[35]A. E. Miroshnichenko, "Off-resonance field enhancement by spherical nanoshells," Phys. Rev. A **81**, 1–5 (2010).
[36]A. Mirzaei, A. E. Miroshnichenko, I. V. Shadrivov, and Y. S. Kivshar, "All-dielectric multilayer cylindrical structures for invisibility cloaking," Sci. Rep. **5**, 9574 (2015).
[37]S. Oldenburg, R. Averitt, S. Westcott, and N. Halas, "Nanoengineering of optical resonances," Chem. Phys. Lett. **288**, 243–247 (1998).
[38]P. Wang, A. V. Krasavin, F. N. Viscomi, A. N. Adawi, J.-S. G. Bouillard, L. Zhang, D. J. Roth, L. Tong, and A. V. Zayats, "Metaparticles: Dressing nano-objects with a hyperbolic coating," Laser Photonics Rev. **12**, 1800179 (2018).
[39]G. V. Naik, B. Saha, J. Liu, S. M. Saber, E. A. Stach, J. M. K. Irudayaraj, T. D. Sands, V. M. Shalaev, and A. Boltasseva, "Epitaxial superlattices with titanium nitride as a plasmonic component for optical hyperbolic metamaterials," Proc. Natl. Acad. Sci. U.S.A. **111**, 7546–7551 (2014).